Author(s): Haarahiltunen, Antti & Varpula, Aapo & Leinvuo, Jouni & Siren, Esko & Rytkönen, Vesa-Pekka & Savin, Hele

Title: Glass Polarization Induced Drift in Microelectromechanical Capacitor

Year: 2012

Version: Final published version

Please cite the original version:

Haarahiltunen, Antti & Varpula, Aapo & Leinvuo, Jouni & Siren, Esko & Rytkönen, Vesa-Pekka & Savin, Hele. 2012. Glass Polarization Induced Drift in Microelectromechanical Capacitor. Journal of Applied Physics. P. 4. 1089-7550 (electronic). DOI: 10.1063/1.4720378

AIP Journal of Applied Physics

Glass polarization induced drift in microelectromechanical capacitor

A. Haarahiltunen, A. Varpula, J. Leinvuo, E. Siren, V.-P. Rytkönen, and H. Savin

Citation: Journal of Applied Physics **111**, 103523 (2012); doi: 10.1063/1.4720378
View online: http://dx.doi.org/10.1063/1.4720378
View Table of Contents: http://scitation.aip.org/content/aip/journal/jap/111/10?ver=pdfcov
Published by the AIP Publishing

Glass polarization induced drift in microelectromechanical capacitor

A. Haarahiltunen,[1] A. Varpula,[1,2] J. Leinvuo,[3] E. Siren,[3] V.-P. Rytkönen,[3] and H. Savin[1]
[1]*Department of Micro and Nanosciences, Aalto University, P.O. Box 13500, FI-00076 Aalto, Finland*
[2]*Microsystems and Nanoelectronics, VTT Technical Research Centre of Finland, P.O. Box 1000, FI-02044 VTT, Finland*
[3]*VTI Technologies Oy, P.O. Box 27, FI-01621 Vantaa, Finland*

(Received 1 December 2011; accepted 18 April 2012; published online 24 May 2012)

We present a quantitative physical model for glass substrate polarization and study the glass polarization by measuring the capacitance drift from microelectromechanical capacitor test structure. The model consists of mobile and immobile charge species, which are related to alkali metals and non-bridging oxygen in glass. The model explains consistently our results and the previously observed non-homogeneous charging effect in a radio-frequency switch fabricated on a glass substrate. The results indicate that the bulk properties of the glass layer itself can be a significant source of drift. The modeling allows estimation of the drift behavior of the several kinds of device structures. © *2012 American Institute of Physics*. [http://dx.doi.org/10.1063/1.4720378]

I. INTRODUCTION

Dielectric charging in a radio-frequency microelectromechanical (RF-MEM) switch is widely studied and identified as one of the major reasons for stability problems.[1–3] Homogenously distributed charges shift the whole capacitance-voltage (C-V) curve.[2] A built-in voltage in a capacitive MEM switch can be determined from the minimum of the C-V curve. Consequently, homogeneous charging of the device can be monitored from the change in the C-V curve minimum. Similarly, a homogenous charging causes a change in both pull-out and pull-in voltages. This can eventually lead to a failure in the operation of the switch, since pull-out might not occur.

Another unwanted effect related to charging is narrowing of the pull-out (or pull-in) window in the C-V curve.[4,5] This can be explained by inhomogeneously distributed charges, which increase the minimum capacitance value and narrow the pull-out (or pull-in) window.[6] This can obviously lead to a failure of the switch if the pull-out window completely disappears. Recently, Czarnecki *et al*. noticed that the narrowing of the pull-out window is related to the substrate the device is fabricated on.[7] Especially an RF switch on glass substrate was prone to inhomogeneous charging.[7] The authors used finite element simulations[7,8] for analyzing the effect of substrate charges, but they did not provide the physical mechanism for the charging of the glass substrate.

In this paper, we present a physical model of charging in a glass substrate. In addition, we present experimental results obtained from a MEM-capacitor test structure and a comparison between modeling and experimental results.

II. EXPERIMENTAL AND THEORY

The sample and the measurement setup are sketched in Fig. 1(a). The samples have two different capacitors. They were fabricated using a modified commercial manufacturing process. The capacitance is measured at 1 MHz across the topmost capacitor (AlCu metallized air gap) using an HP-4192 A impedance analyzer. The bottom capacitor, which does not contain a metal layer, is used for studying the charging (i.e., polarization) of the glass. The bottom capacitor is DC-biased using a Keithley 237 source-measure unit. The DC-bias voltage causes the space-charge polarization of the glass and changes the electrostatic force in the bottom air-gap, which can be detected as a change in the capacitance of the metallized gap. The thicknesses of the glass and the air gaps are 100 μm and 1 μm, respectively.

The capacitance changes were measured in the 20–80 °C temperature range. At each temperature point, the DC-bias voltage was varied sequentially (0 V, 4 V, 0 V, −4 V, 0 V). Due to the thermal activation of the polarization, the duration of each DC-bias stress point was gradually decreased when temperature was increased.

In order to analyze theoretically the glass polarization, we use an approximative 1D model (Fig. 1(b)) and the single mobile ion model,[9] which can be described mathematically using the continuity equation

$$\frac{\partial p}{\partial t} = D\frac{\partial^2 p}{\partial x^2} - \mu\frac{\partial}{\partial x}(Ep) + q - a, \tag{1}$$

where p is the concentration of mobile uncombined positive charges, D is the diffusion constant of positive charges, μ is the mobility of the positive charges, E is the electric field, q is the dissociation rate, and a is the recombination rate. Einstein's relation, $D/\mu = kT/q$, is assumed to hold here. The electric field can be solved from Poisson's equation using the total voltage drop as the boundary condition

$$\frac{\partial E}{\partial x} = \frac{q(p-n)}{\varepsilon_g \varepsilon_0} \quad V_{bias} = \int_0^{t_g+g} E dx, \tag{2}$$

where ε_g is the relative permittivity of glass, ε_0 is the electric constant, n is the concentration of immobile negative charges, t_g is the thickness of glass, and g is the thickness of the air gap. The recombination rate is assumed to be proportional to the product of the negative and positive charge concentrations. Similarly, the dissociation rate is assumed to be proportional to the undissociated charge concentration[9]

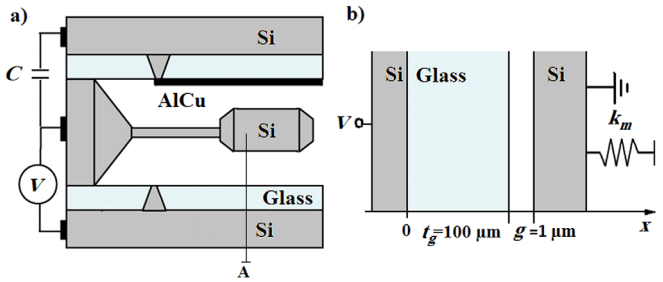

FIG. 1. (a) A schematic picture of the MEM sample cross-section and the measurement setup. (b) One-dimensional model of the air gap of the MEM system employed in the analysis of the glass polarization (line A). t_g is thickness of the glass layer, and g is the air gap. The glass substrate is made from Schott Borofloat 33.

$$a = \alpha np \quad q = \kappa(c - n), \tag{3}$$

where c is total concentration of chemical species that can thermally dissociate creating a pair of positive and negative charges. α and κ are recombination and generation rate constants, respectively.

III. RESULTS AND DISCUSSION

The experimental results at 50 °C and 80 °C are shown in Fig. 2. The strong temperature dependency is clearly visible. Shih *et al.* showed that during anodic bonding, most of the bonding voltage will drop very quickly (in few tens of milliseconds) across the air gap at a high temperature.[10] They solved analytically the single mobile ion model without diffusion, generation, and recombination and found that the time constant of this connection is proportional to the resistivity of glass.[10] The resistivity of glass is strongly temperature-dependent. This explains the fact that temperature had a remarkable effect on the timescale of the capacitance drift in our measurements. During the first 4 V DC-bias point, the capacitance changes rather linearly with time. The reason for linear change can be explained in a general manner as in the beginning of transient $\exp(-t/\tau) \approx 1 - t/\tau$. Herfst *et al.* explained similarly observed square root time dependency as a short time approximation of stretched exponential $\exp(-t^{1/2})$.[11] The capacitance drift at 4 V in Fig. 2 stops because the silicon mass hits the mechanical stopper, but charges are still far away from the equilibrium. The Arrhenius plot of the absolute value of the rate of the capacitance change during the first 4 V DC-bias point is shown in Fig. 3. The result corresponds to the activation energy of 0.9 eV, which is in agreement with the activation energy of 1.0 eV determined for the glass conductivity.[12] The results in Fig. 3 were measured from the same device. There was a long time delay at 0 V bias (much longer than shown in Fig. 2) before starting the measurement to ensure a well-defined initial condition for the first 4 V transient. This was also the reason for choosing the first transient for the activation energy analysis.

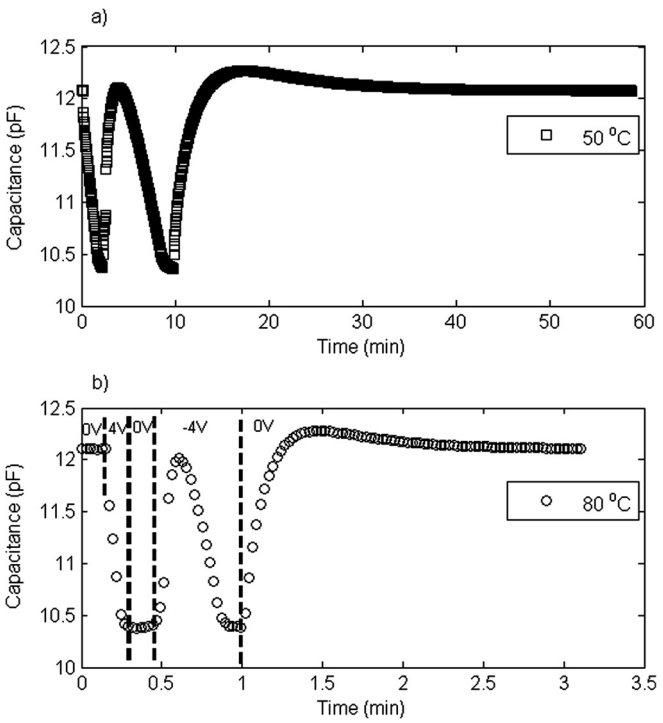

FIG. 2. The measured capacitance as a function of time at (a) 50 °C and (b) 80 °C. The bias voltage sequence of 0, 4, 0, −4, 0 V is indicated in (b). The duration of each DC-bias stress point was controlled so that the magnitudes of the changes in the capacitance were the same at both temperatures.

For further analysis of our experimental results, we combine the theoretical results from Ref. 1 and the single mobile ion model. The electrostatic force in the biased air gap can be calculated as[1]

$$F_{el} = A\varepsilon_0 \left(\frac{\varepsilon_g}{\varepsilon_g g + t_g} \right)^2 (V_{bias} - V_{bi})^2, \tag{4}$$

where A is area of the beam and V_{bi} is the built-in voltage, which can be calculated from the charge distribution[1]

$$V_{bi} = V_0 + \frac{1}{\varepsilon_g \varepsilon_0} \int_0^{t_g} x(p + n)dx, \tag{5}$$

where V_0 is typically caused by a Fermi-level difference of two dissimilar materials. Here, V_0 can also be the band-bending difference between the beam and the bottom silicon

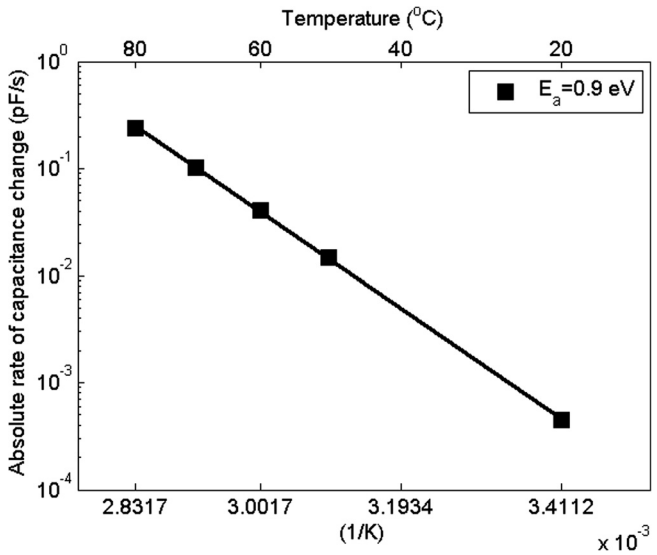

FIG. 3. The Arrhenius plot of the drift rate of capacitance during the first 4 V DC-bias.

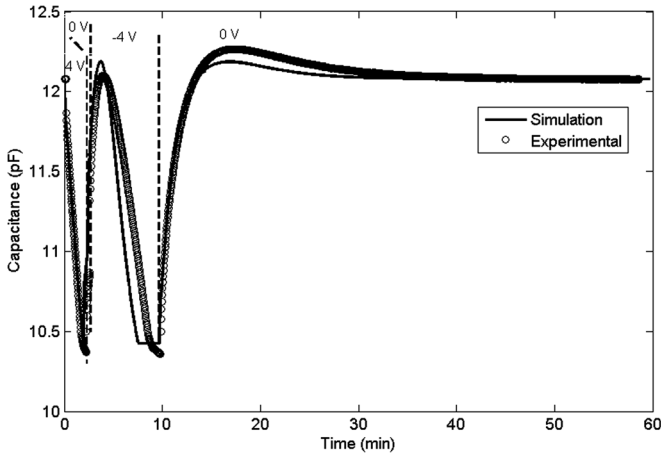

FIG. 4. Comparison of experimental and simulation results at 50 °C.

related to the electric charge. The band bending remains practically constant in the voltage ranges employed in the experiments, since the doping level of silicon is high ($>10^{17}\,\mathrm{cm}^{-3}$). A value of $V_0 = 0.4\,\mathrm{V}$ was employed in the simulations, and the silicon surfaces were assumed to be metallic in behavior.

The comparison between our experimental and simulation results is presented in Fig. 4. In the simulations, $\varepsilon_g = 4.6$ was used.[12] The air-gap voltage was calculated using Eqs. (1) and (2) with small time steps. After each time step, the air gap was recalculated from Eqs. (4) and (5) using the experimentally determined effective spring constant, $k_{eff}\Delta g = F_{el}$. The resistivity was adjusted by fitting the slope of the capacitance during the first 4 V DC-bias sequence (see Fig. 4). Numerical simulations also confirm the linear dependency and the assumption that charges are far from equilibrium when silicon mass hits the mechanical stopper. This gave a resistivity of 5.4×10^{13} Ωcm for the glass, which is slightly smaller than the value of 1.2×10^{14} Ωcm suggested by the datasheet.[12] The resistivity of the glass layer is determined by the mobility and concentration of the mobile charge. We noticed that a better qualitative fitting of the experimental result in Fig. 4 can be obtained using a low concentration of charge, $4 \times 10^{12}\,\mathrm{cm}^{-3}$. The low concentration range is important because only a very small fraction of total alkali cations is typically mobile at low temperature.[13]

The simulation results shown in Fig. 4 reproduce the experimental behavior relatively well. Figs. 2 and 4 show that the direction of the drift changes, although the DC-bias voltage is kept constant. This simply means that an electrostatic force passes through a minimum value, i.e., the built-in voltage (see Eq. (4)) changes its sign. The main difference between the simulations and the experiments is that the peaks of the simulated capacitance curves have the same value (see Fig. 4), while in the experimental curves, the peak capacitance seems to increase with time. This and the other small discrepancies can be explained by 2D effects, i.e., the air gap is not laterally constant, and charges also spread laterally in the glass, which affects the electrostatic force in the air gap. In the simulations, we neglected generation and recombination since their effect on the simulations was not relevant.

The glass polarization under a DC-bias voltage can clearly explain the non-contact drift and the narrowing of the pull-in (or pull-out) window observed in Refs. 7 and 8. In addition, it is known that humidity affects sodium and hydrogen concentrations in the glass surface layer.[14] This and our model explain the reduced lifetime of a switch built on a glass substrate observed after storage in air ambient.[8] The evaporation of water by short annealing does not improve the lifetime of these glass-substrate switches,[8] since the water on the glass surface causes long-range changes due to diffusion of ions.

The polarization of the dielectric is an intrinsic property and may occur without charge injection,[15] which is a clear difference as compared to other charging models.[8] The intrinsic properties of glasses may change with chemical composition, but the results presented here are applicable as long as the electrical current flow is due to ionic conduction because the space charge separation is the slowest polarization mechanism. It is also known (e.g., Ref. 16) that even though glass is ideally free of alkali metals, the sodium contamination can be high enough to contribute to the space charge polarization. Of course, the mobile ionic contamination problem is not limited to glass but concerns all dielectrics used in MEM system processes. The mobile ionic contamination might even be the dominating effect in devices operating at rather low electric fields.[17,18]

IV. CONCLUSIONS

Our results clearly indicate that glass is prone to space charge polarization during DC-bias stress. This property makes glass practical material in anodic bonding, e.g., in hermetic sealing. On the other hand, this can cause a long-term drift at low temperatures in a MEM capacitor, although this glass can still be used to form stable capacitors and low-loss substrates at higher frequencies. Fortunately, this harmful effect can be modeled (and therefore minimized) rather easily by knowing the glass resistivity and its temperature dependency, as shown here. The modeling enables the design of devices with a minimal drift from the glass substrate and separation of the space charge polarization induced drift from the other charging mechanisms.

ACKNOWLEDGMENTS

A. Haarahiltunen, H. Savin, and A. Varpula acknowledge the financial support from the Academy of Finland. The VTI Technologies are acknowledged for providing samples for the experiments.

[1]W. van Spengen, R. Puers, R. Mertens, and I. De Wolf, J. Micromech. Microeng. **14**, 514 (2004).
[2]J. Wibbeler, G. Pfeifer, and M. Hietschold, Sens. Actuators A **71**, 74 (1998).
[3]C. Goldsmith, J. Randall, S. Eshelman, T. H. Lin, D. Denniston, S. Chen, and B. Norvell, in *IEEE MTT-S International Microwave Symposium Digest*, edited by R. G. Ranson (IEEE Microwave Theory and Techniques Society, San Francisco, California 1996), Vol. 2, pp. 1141–1144.
[4]J. R. Reid and R. T. Webster, Electron. Lett. **38**, 1544 (2002).
[5]Z. Olszewski, R. Duane, and C. O'Mahony, Appl. Phys. Lett. **93**, 094101 (2008).
[6]X. Rottenberg, I. De Wolf, B. Nauwelaers, W. De Raedt, and H. Tilmans, J. Microelectromech. Syst. **16**, 1243 (2007).
[7]P. Czarnecki, X. Rottenberg, P. Soussan, P. Ekkels, P. Muller, P. Nolmans, W. De Raedt, H. A. C. Tilmans, R. Puers, L. Marchand, and I. DeWolf, Sens. Actuators, A **154**, 261 (2009).

[8]P. Czarnecki, "Impact of charging mechanisms on the reliability of RF MEMS devices," Ph. D. dissertation (Arenberg Doctoral School of Science, Engineering & Technology, Faculty of Engineering, Department of Electrical Engineering, Katholieke Universiteit Leuven, Leuven, Belgium, 2010).
[9]T. M. Proctor and P. M. Sutton, J. Chem. Phys. **30**, 212 (1959).
[10]W. P. Shih, C. Y. Hui, and N. C. Tien, J. Appl. Phys. **95**, 2800 (2004).
[11]R. W. Herfst, P. G. Steeneken, and J. Schmitz, in *Proceedings of 45th Annual International Reliability: 417 Physics Symposium, Phoenix* (IEEE Electron Device Society and Realibility Society, 2007), p. 417.
[12]See http://www. schott.com/borofloat/english/download/borofloat_33_e.pdf for Datasheet of Schott Borofloat® 33 glass.
[13]J.-L. Souquet, M. L. F. Nascimento, and A. C. M. Rodrigues, J. Chem. Phys. **132**, 034704 (2010).
[14]R. H. Doremus, Y. Mehrotra, W. A. Landford, and C. Burman, J. Mater. Sci. **18**, 612 (1983).
[15]G. J. Papaioannou, G. Wang, D. Bessas, and J. Papapolymerou, in *Proceedings of European Microwave Conference* (European Microwave Association, Manchester, UK, 2006), pp. 1739–1742.
[16]E. H. Snow and M. E. Dumesnil, J. Appl. Phys. **37**, 2123 (1966).
[17]A. Haarahiltunen, A. Varpula, and H. Savin, J. Appl. Phys. **110**, 043505 (2011).
[18]G. Bahl, R. Melamud, B. Kim, S. A. Chandorkar, J. C. Salvia, M. A. Hopcroft, D. Elata, R. G. Hennessy, R. N. Candler, R. T. Howe, and T. W. Kenny, J. Microelectromech. Syst. **19**, 162 (2010).